An Experimental Investigation of Rapid Depressurization Extinguishment

G. E. JENSEN* AND R. S. BROWN†
United Technology Center, Sunnyvale, Calif.

Results are presented from an experimental study of solid propellant extinguishment by rapid depressurization. Systematic variations in propellant binder, oxidizer loading level, burning rate catalyst, metal loading, and exhaust pressure level were studied. The effects of motor configuration on extinguishment and reignition are discussed. Results indicate that combustion extinguishment requirements are determined by the binder type, percentage of ammonium perchlorate oxidizer, motor geometry, and exhaust pressure level as well as the pressure and depressurization rate. The von Elbe model with a coefficient of one provides a rough correlation of extinguishment requirements.

Nomenclature

AP	=	ammonium perchlorate
b.out	=	grain burned out
CTPB	=	carboxy terminated polybutadiene
CTPIB	=	carboxy terminated polyisobutylene
dP/dt	=	depressurization rate
DSC	=	differential scanning calorimeter
HYCAT	=	proprietary catalyst
L^*	=	motor volume/throat area
n	=	burning rate exponent
P	=	pressure
PBAN	=	polybutadiene-acrylic acid-acrylonitrile
$\dot{P}$	=	depressurization rate
PU	=	polyurethane
$\dot{r}$	=	transient burning rate
$\bar{r}$	=	steady-state burning rate
Reig.	=	grain reignited
S	=	swing-nozzle motor
t	=	time
α	=	thermal diffusivity
λ	=	const
ω	=	window motor
ωv	=	window motor vacuum exhaust

Introduction

DURING the past few years, significant effort has been directed toward evaluations in the field of $\dot{P}$ and L^* induced combustion extinguishment of solid propellants. The majority of these studies have been directed toward establishment of the depressurization rate required for extinguishment of different propellants. In general, these studies[1-3] have not provided the necessary insight into the mechanisms of combustion termination nor a sound basis for engineering correlations to permit the design of controllable solid propellant motors. Data have been particularly lacking for a quantitative description of transient combustion phenomena, the predictability of the actual point of combustion extinguishment, the mechanisms of the extinguishment processes, and the factors which control possible reignition of the grain.

Presented as Paper 70-665 at the AIAA 6th Propulsion Joint Specialist Conference, San Diego, Calif., June 15–19, 1970; submitted September 21, 1970; revision received June 1, 1971. This work was supported by NASA/Langley under Contract No. NAS 1-7815.

* Senior Research Engineer, Combustion Research Section, Propulsion Research Branch. Member AIAA.

† Chief, Combustion Research Section, Propulsion Research Branch. Member AIAA.

Theoretical efforts to describe transient combustion and extinguishment phenomena have shown the complexity of the process. One major impediment in describing transient combustion behavior is the lack of basic information in the description of propellant-ingredient decomposition mechanisms, gas-phase mixing of decomposition products, and gas-phase combustion kinetics under both steady-state and transient combustion conditions. Simple transient combustion models[4-6] shown in general form in Eq. (1), are based on a simple surface energy balance, the assumption of a constant surface temperature, and the use of an empirical description of steady-state combustion behavior.

$$\dot{r} = \bar{r}[1 + (1/\lambda)(n\alpha/r^2)(1/P)(dP/dt)] \quad (1)$$

where $\dot{r}$ = transient burning rate, $\bar{r}$ = steady-state burning rate at pressure P, n = burning rate exponent, α = thermal diffusivity, and λ = const ($\frac{1}{2}$,1,2.0). As predicted by the von Elbe-type model previously mentioned, the transient burning rate is always less than the steady-state burning rate at any pressure during transient combustion. The conditions required for extinguishment are determined by equating $\dot{r}$ to zero. The wide range of values for the constant λ as well as the simplifying assumption underlying the model make it difficult to use this model for a priori design.

More complex transient combustion models[7-9] which are based on the assumption of an Arrhenius-type regression rate expression also have been formulated. In solving these models for a particular depressurization path, the surface temperature is allowed to vary in contrast to solutions of the von Elbe-type model. If the propellant surface temperature falls below an arbitrary limit[9] or if the gas phase kinetics are quenched[8] combustion extinguishment is said to be achieved. These models are probably more realistic and have a greater potentiality for describing the effects of propellant formulation differences; but in their present form they are of limited usefulness, primarily because of a lack of propellant kinetics understanding.

Particularly lacking for design purposes are experimental data which specify 1) the conditions of propellant extinguishment (the pressure and depressurization rate at extinguishment), 2) the effect of propellant differences upon extinguishment condition, 3) the perturbing influence of exhaust pressure upon extinguishment and permanence of extinguishment, and 4) the effect of motor differences upon extinguishment behavior. The following sections of this paper are the result of an experimental program[10] to elucidate these four areas.

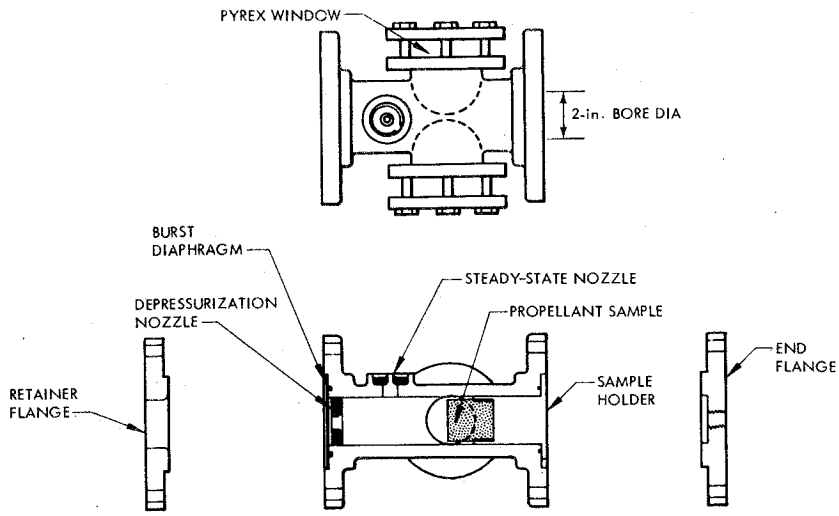

Fig. 1 Schematic of window motor.

Experimental

Depressurization studies were conducted using two depressurization or $\dot{P}$ motors. A relatively large volume, dual-nozzle window motor was used for high-speed film studies, propellant formulation evaluation and for the study of the effect of exhaust-pressure level upon extinguishment and reignition behavior. A tubular, internal-burning grain swing nozzle motor was used for the study of motor differences.

Window Motor

The windowed motor shown schematically in Fig. 1 was used for both rapid depressurization and L^* extinguishment studies. The motor has a dual-nozzle system with a top mounted nozzle for steady-state operation and a nozzle of the aft end for either depressurization of the motor or L^* operation. In conducting L^* tests, the upper nozzle is plugged and the termination nozzle serves as a steady-state nozzle. Both the $\dot{P}$ and L^* grains can be viewed through the 1-in. thick tempered Pyrex windows mounted on the sides of the motor.

Depressurization of the motor was achieved either by using a brass burst disk, needle assembly mounted aft of the depressurization nozzle or by using a composite mylar, brass disk assembly mounted downstream of the termination nozzle. In using the latter system, a nichrome heater wire was placed around the unrestrained periphery of the mylar disk and connected to a voltage supply. Upon command, the wire was heated electrically causing first the mylar disk to fail and secondly the brass disk to burst depressurizing the motor. This system was used to permit the motor to be mated to a 1000-liter vacuum tank for exhaust pressure level studies.

While a variety of grain geometries can be used with this motor the depressurization studies were conducted using neutral burning 1-in. wide by 5-in. long grains. Ignition was achieved with an oxygen-methane igniter firing for 0.25 sec. With the neutral burning grain in place the motor has a volume of 22 in.^{3}

Instrumentation for the propellant characterization tests consisted of two Texas Instrument LS-223 photovoltaic light sensors and two strain-gage pressure transducers. Signals from these instruments were recorded on a CEC 124 oscillograph using 7-319 galvanometers and a recording chart speed of 64 in./sec.

Swing-Nozzle Motor

The motor shown in Fig. 2 was utilized with the window motor to achieve $\dot{P}$ data over a wide range of operating conditions. As shown, the internal-burning grains used in the motor can either be restricted on the ends of the grain or left unrestricted, giving a moderately progressive burning trace. The grains had an initial port diameter of 0.5 in. and thus, provided up to 2 sec of burn time. Two grain lengths of 5- and 15-in. grains were used for the swing-nozzle motor tests. The 5-in.-long grains had a burnout volume of 10 in.^{3}, and the 15-in.-long grains had a burnout volume at 27.7 in.^{3} In general, the volumes at termination were 4 and 9.1 in.^{3}, respectively.

The motor was ignited using a methane/oxygen hot-gas igniter firing for 0.5 sec. After ignition and a burn time of 0.7–1.0 sec, the motor was depressurized by releasing the downstream graphite steady-state nozzle which is mounted in a swing-nozzle assembly. The assembly was released upon command by exceeding the tensile strength of the single, notched bolt used to restrain the assembly during steady-

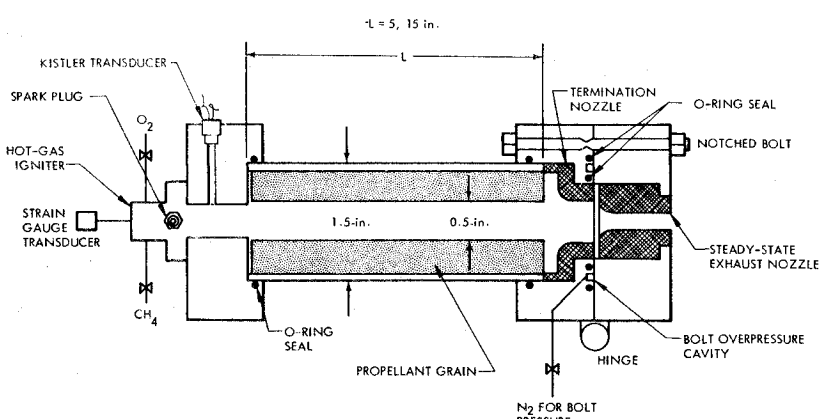

Fig. 2 Schematic of swing wing-nozzle motor.

state operation. This was accomplished by pressurizing the space between two O-rings mounted on the aft face of the motor between the nozzle assembly and the motor body. The restraining bolt was sized to fail when the force caused by pressurization was equal to that force exerted on the door by the motor gases.

The rate of depressurization of the motor was controlled by a large diameter nozzle assembly mounted at the aft end of the grain. As shown in Fig. 2, this assembly consisted of a copper nozzle retainer and a graphite nozzle. The nozzle was mounted close to but not touching the aft end of the grain to minimize reignition problems.

Instrumentation for this motor consisted of a Kistler 601-A quartz pressure transducer, a Statham strain-gage pressure transducer, and a Solar System 300-2 light sensor. The pressure transducers were mounted at the head end of the motor. Data were recorded at 80.0 in./sec on a CEC oscillograph using a 7-326 galvanometer for recording the Kistler transducer signal and 7-342 galvanometers for the other transducer signals. A conventional sequence unit was used for control of the entire firing and depressurization cycle.

Propellants

Four basic formulation variables were evaluated in the course of the program: 1) binder-polymer-curative variations, 2) AP loading level and size distribution, 3) aluminum loading level, and 4) catalyst content. The effect of binder composition upon $\dot{P}$ extinguishment behavior was studied using CTPB, PU, and CTPIB binder systems. In addition, several chlorinated binders based on the CTPIB system and a sterilized CTPIB system were studied. CTPIB binders containing 1.2% (wt-% of binder), 3.4 and 14.5% chlorine were studied to determine if such halogens would reduce the $\dot{P}$ requirements of the CTPIB system. The propellants used for the binder studies contained 83.8% AP with a 65:35 coarse to fine ratio, 0.2% carbon black and no aluminum. The coarse AP had a mean particle diameter of 190 μ and the fine AP had a mean diameter of 6.3 μ.

The CTPIB, CTPB, and polyurethane propellants were selected for study because of the diverse thermal and oxidative degradation characteristics of the binder polymers. Limited studies[11-13] indicate that the more easily terminated polyurethane and CTPIB formulations are less subject to exothermic oxidative degradation of the binder and are more easily degraded by endothermic thermal decomposition. The CTPB polymer shows greater susceptibility to oxidative degradation, is less subject to thermal degradation, and has a higher flame temperature which may contribute to greater heat feedback from gas-phase combustion.

DSC studies conducted during this program, along with concurrent studies by Shannon[14] demonstrated the differences of the thermal decomposition of the three binders. At a heating rate of 10°C/min. and a 3.1 mg sample of CTPB binder in nitrogen, first decomposition (endothermic) was noted at 303°C, and sample darkening was observed at 390°C. Bubble formation within the sample occurred at 450°C, followed by rapid fume-off at 470°C. Decomposition was complete at 491°C with a 0.05-mg residue remaining.

Under similar conditions polyurethane was observed to melt at 215°C and decomposition was complete at 397°C. Decomposition of CTPIB first resulted in droplet formation on the viewport at 153°C. The sample melted between the range of 240–269°C. Bubble formation began at 280°C and rapid fume-off occurred from 300° to 350°C. Decomposition was complete at 419°C.

The effect of oxidizer loading level upon extinguishment behavior was explored using variations of the CTPB system, while the effect of coarse to fine ratio was explored with the CTPIB propellant system. Four metallized noncatalyzed formulations were $\dot{P}$ characterized in the course of the program—two CTPB formulations containing 4 and 16% aluminum in place of AP and two similar CTPIB propellants.

The effect of burning rate catalyst upon the extinguishment behavior of the CTPB system was studied with two nonmetallized and two aluminized propellants. The two nonmetallized CTPB propellants contained, respectively, 0.25% iron oxide and 0.25% organo-iron catalyst and 83.8% AP. The two aluminized propellants contained 16% aluminum and 3 and 1% HYCAT, respectively, with a total solids loading of 84%. The effect of burning rate catalyst addition to the CTPIB system was studied with one formulation containing 0.25% organo-iron catalyst and 83.8% AP with no aluminum and a second formulation containing 1% HYCAT, 16% aluminum, and 68% AP. The addition of iron oxide or organo-iron catalyst at the 0.25% level had a moderate effect upon the burning rate of the CTPB and CTPIB propellants at both 15 psia and higher pressures (20–33% increase). The addition of 1 or 3% HYCAT markedly increased the burning rate at all pressure levels (~75% increase at 15 psia with 1% HYCAT, 50% increase at 1000 psia with 1% HYCAT).

Results

Using as a basis of comparison the minimum initial depressurization rate of the motor at a given initial chamber pressure it was found that the binder type, motor geometry, and exhaust pressure level had marked influence upon extinguishability of the different propellants. Using the window motor, it was found that the CTPB propellants were most difficult to terminate and that the critical depressurization rate required for extinguishment was dependent upon the exhaust pressure level. The PU formulation was less difficult to terminate and the extinguishability requirements also were found to be a function of exhaust pressure level. When the motor was fired into the atmosphere at 14.7 psia, the initial or critical depressurization rate required for extinguishment was greater than when the motor was fired into the vacuum tank. The CTPIB formulations had the lowest extinguishment requirements and extinguishment was found to be independent of exhaust pressure. It was also found that the critical depressurization rates with the smaller volume larger grain area swing-nozzle motor were significantly higher than the rates found for all three types of propellant with the window motor.

The addition to the CTPIB system of halogens at low concentrations had little or no effect upon extinguishment behavior. Three chlorinated CTPIB propellants containing 1.2, 3.4, and 14.5% of chlorine (percentage of binder prepolymer which constitutes 12.55% of the propellant) were tested with the dual-nozzle window motor and were found to have nearly the same extinguishment requirements as the reference, nonchlorinated propellant.

The substitution of aluminum for AP in either CTPB or CTPIB propellants decreased the termination requirements, although the tendency for reignition appeared to be more pronounced. Tests were conducted with 4 and 16% aluminum-loaded CTPB and CTPIB propellants. The substitution of 4% aluminum for AP in both types of propellant caused a slight reduction of the critical extinguishment limits, and the substitution of 16% aluminum for AP caused a definite reduction of the critical extinguishment requirements. These effects were most noticeable under vacuum exhaust conditions. When the motors were exhausted into the atmosphere, reignition of extinguished grains often occurred, particularly with tests conducted using the swing-nozzle motor. A wide band of reignition limits was noted for the aluminized propellants tested in the swing-nozzle motor. However, it was shown that reignition could be prevented by the use of a nitrogen purge flowing through the motor immediately after depressurization. The wide reignition limits of the nonpurged motors indicate a

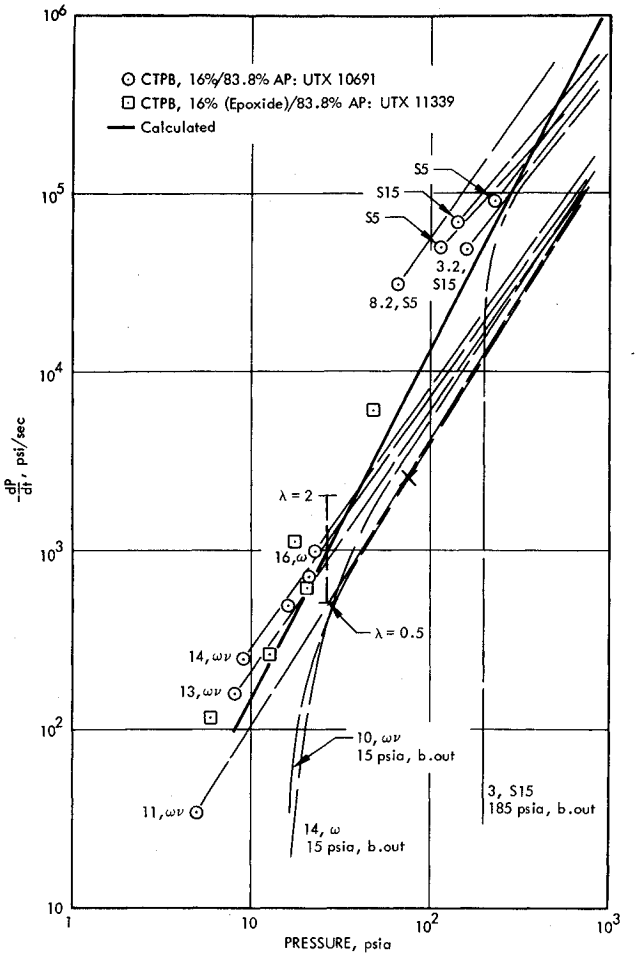

Fig. 3 Comparison of calculated and experimental extinguishment requirements for CTPB/83.8% AP propellant.

serious potential problem for atmospherically depressurized motors.

The addition of burning rate catalysts to a propellant had little or no effect upon the extinguishment requirements in the large-volume, small-grain area motors used in this program. It is conceivable that the increased burning rates would necessitate increased termination requirements in smaller volume (or larger grain-area) motors. This area requires further study. The addition of HYCAT catalysts to the CTPB and CTPIB 16% aluminum propellants greatly increased the reignition limits of grains depressurized at atmospheric exhaust. Initial depressurization rates, an order of magnitude greater than required for extinguishment under vacuum exhaust conditions, were needed to achieve permanent extinguishment when the motors were exhausted into the atmosphere. Examinations of the propellant grains terminated under vacuum conditions showed a heavy layer of agglomerated aluminum on the quenched grain surfaces.

The results obtained with the window motor showed that the exhaust pressure level affected the ease of extinguishment of the propellants prepared using CTPB or polyurethane binder systems. However, exhaust level was found not to influence the behavior of the majority of the CTPIB propellants. The exhaust level effect indicates that combustion extinguishment of the polyurethane and CTPB propellants in the window motor must have occurred after the nozzle dechoked during depressurization to atmospheric exhaust (pressures less than 25–30 psia). Alternately, combustion of the CTPIB propellants must have terminated at higher pressures since the dechoking had little or no influence upon the termination process. It was also apparent that extinguishment in the swing-nozzle motor occurred at much higher pressures and depressurization rates than in the window motor. This was verified by examination of the data traces. If combustion extinguishment was achieved in the window motor, a definite break in the pressure trace (and the light sensor trace) could generally be discerned. This break was taken to be the point of actual combustion termination or the point at which propellant regression stopped, thus causing an abrupt change in the depressurization of the motor. The pressure at extinguishment was less for the CTPB and polyurethane propellants than for the CTPIB systems. Determination of the point of extinguishment using the swing-nozzle motor was harder because of the much greater depressurization rates and the fact that extinguishment occurred at much higher pressure levels. If the grain did not terminate, burnout occurred at a much higher pressure in the swing-nozzle motor than in the window motor; this observation reinforced the fact that extinguishment occurred at higher pressure. In order to achieve permanent extinguishment, it was necessary that the grain be terminated at a pressure above the burnout pressure. Further confirmation of the different extinguishment pressures was obtained by examination of the aluminized propellant grains extinguished in the two motors. As noted previously, the surfaces of the grains extinguished in the window motor were covered with an extensive network of sintered aluminum balls. A smaller quantity of balls was found on the grains extinguished in the swing-nozzle motor. In all probability, the extensive aluminum network on the window motor grains was formed during low-pressure deflagration, e.g., during the depressurization cycle. The lack

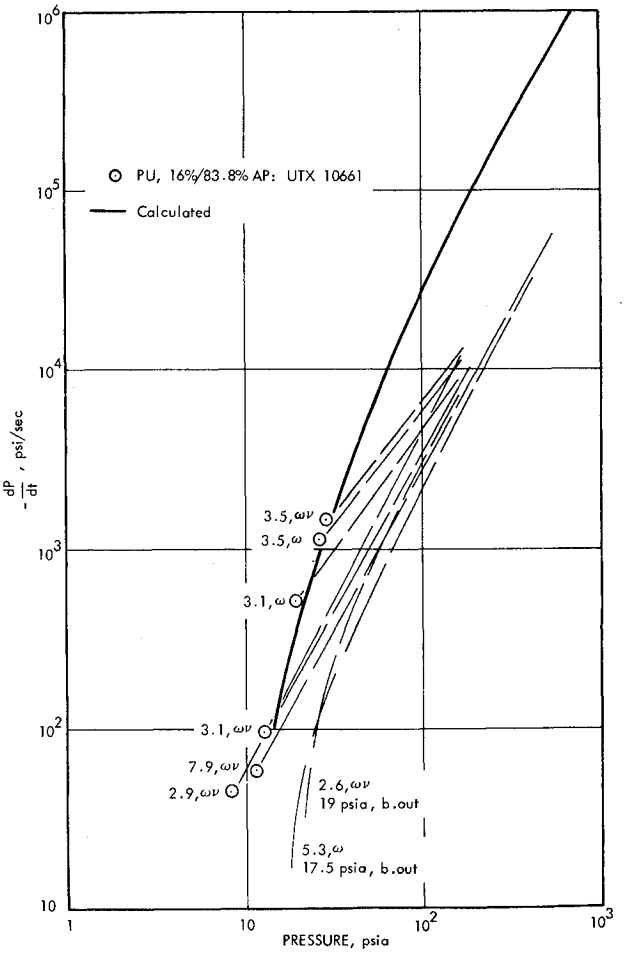

Fig. 4 Comparison of calculated and experimental extinguishment requirements for PU/83.8% AP propellant.

of aluminum deposition on the swing-nozzle motor grains is indicative of combustion extinguishment at higher pressures.

In general, the experimental depressurization paths were described by a simple exponential decay function, but a number of traces did show one or more changes in slope during depressurization. The step change of the depressurization rate was also matched by a change of the light sensor signal intensity. In some instances these disturbances were possibly the result of aluminum sluffing; however, a number of tests conducted with the nonaluminized propellants showed both depressurization rate and light sensor discontinuities. This type of behavior was most prevalent with the 79.8% AP-loading CTPB propellant, UTX 11327.

Another type of behavior was observed occasionally during tests with the swing-nozzle motor. Upon depressurization the motor pressure fell to a level above the exhaust pressure and then quickly recovered to a still higher burnout pressure. In general, two or three cycles of unstable combustion were also noted during this recovery period. A similar type of behavior was observed with the window motor; however, the time scale was much longer (1–2 sec) and the grains generally terminated after the pressure rose and then fell for the second time.

To present the data obtained in the course of the program and to provide a means of interrelating the results derived using the different motors, the data were correlated on the basis of the depressurization paths during blowdown. The data are shown in Figs. 3–6, wherein the dashed lines represent the depressurization paths of the majority of tests performed. The depressurization rates during blowdown are plotted in logarithmic form on the ordinate, and the abscissa represents the logarithmic pressure level at any depressurization rate. The upper end on each of the dashed lines represents the initial depressurization rate and the initial or steady-state pressure. The lower end of each line represents the depressurization rate and pressure at combustion extinguishment, if extinguishment occurred. In the event the grain burned out, the lines have been plotted asymptotically to the burnout pressure. For clarity, only the pressure and depressurization rate at the point of extinguishment are represented for the majority of the tests shown. The various constants and experimental parameters shown in these figures are explained in detail as follows: dP/dt = depressurization rate, instantaneous; P = instantaneous pressure during depressurization; λ = theoretical constant; S5 = 5-in. long swing-nozzle motor; S15 = 15-in. long swing-nozzle motor; ω = window motor, atmospheric exhaust; $\omega\nu$ = window motor, vacuum exhaust.

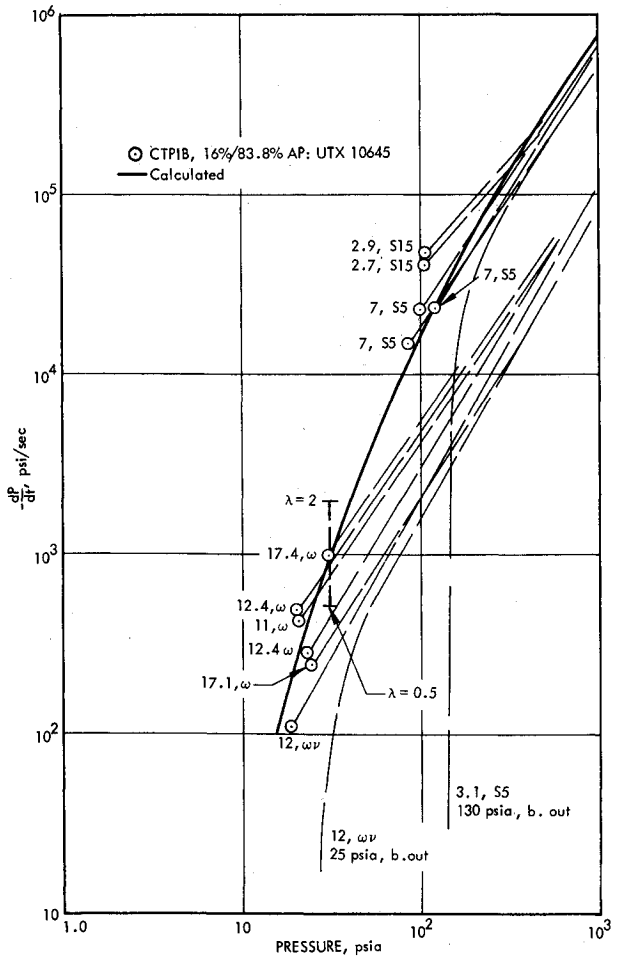

Fig. 5 Comparison of calculated and experimental extinguishment requirements for CTPIB/83.8% AP propellant.

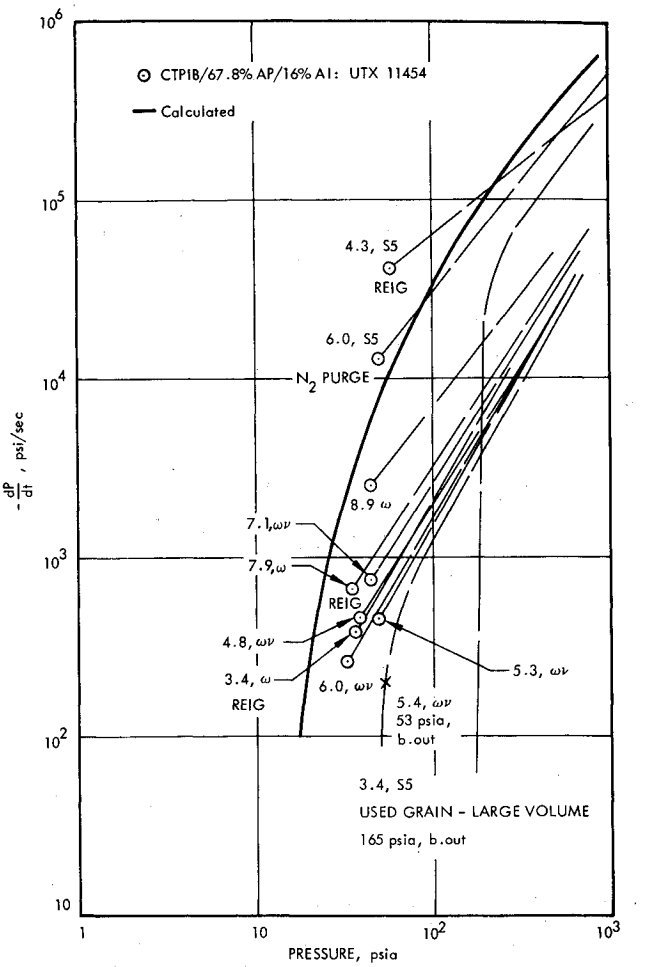

Fig. 6 Comparison of calculated and experimental extinguishment requirements for CTPIB/AP/16% aluminum propellant.

In general, it was found that, if extinguishment occurred, the extinguishment depressurization paths could be adequately represented by a straight line on logarithmic coordinates. However, occasionally the depressurization paths showed a step change in depressurization rate. This characteristic was often observed with the CTPB/79.8% AP formulation.

Also shown in Figs. 3–6 are the extinguishment requirements calculated by use of the von Elbe-type model. Extinguishment is predicted when $dP/dt = -\lambda P\dot{r}^2/n\alpha$ where λ may have a value of 0.5, 1.0, or 2.0, depending upon the particular model of combustion extinguishment. For comparison purposes the line $dP/dt = -P\dot{r}^2/n\alpha(\lambda = 1)$ has been plotted for each of the propellants tested. Because all

burning rates could not be described by a power law expression, some of the calculated solid lines are not straight lines. For the calculated limits, n and $\bar{r}$ were taken from the strand burning data while α, the thermal diffusivity, was taken as 2.5 10^{-4} in.^{2}/sec for the nonaluminized propellants and 3.0 10^{-4} in.^{2}/sec for the aluminized propellants.

The possible bounds of the calculated extinguishment conditions with $\lambda = 0.5$ to $\lambda = 2.0$ are shown in Fig. 3. These limits are greater than the errors which may result from a lack of knowledge of the thermal properties of the propellants. The most important factor in the calculated expression is the propellant burning rate at any specified pressure.

Discussion

An examination of the results presented in Figs. 3–6 shows a fair agreement between the experimental and calculated extinguishment conditions. The calculated and experimental requirements were more in agreement when the window motor was used than when the swing-nozzle motor was used. However, this may be because of the greater uncertainty of the swing-nozzle motor data.

Whether the agreement between the calculated and experimental data provides experimental confirmation of the theory or is merely fortuitous is open to speculation. The possible bounds on the calculated results are quite large, as indicated in Fig. 3. It should also be noted that requirement for combustion extinguishment, i.e., $dP/dt = -\bar{r}^2P/n\alpha$, can be obtained either from a model which considers only processes occurring in the solid phase[4,5] or only processes occurring in the gas phase.[6] Examination of the data of Fig. 5 and particularly Fig. 6 shows little variation of the extinguishment pressure over a wide range of depressurization rates. The extinguishment pressure is nearly constant. This type of behavior also was observed by von Elbe and McHale.[3]

There are qualitative trends in the data which can be noted from these correlations. The conditions required for experimental extinguishment of the CTPB propellants range from more severe than, to equal to the calculated conditions. Conversely, the conditions for experimental extinguishment of the CTPIB propellants are equal to, or less than the calculated requirements. Though not shown, reducing the AP loading level of the CTPB propellant reduced the requirements for extinguishment of the CTPB propellant and provided better agreement with the calculated values.

Based on these trends, it is evident that the binder composition has a definite influence upon the ease of extinguishability. It is reasonable that the thermal decomposition behavior of the binder system will influence extinguishability. Shannon[15] showed that these propellants, formulated with binders which thermally degraded at lower temperatures (CTPIB), are harder to ignite at lower-pressure levels than propellants formulated with more thermally stable binders (CTPB and PBAN). Also, as the endothermicity of the propellant was increased by increasing the binder level, the ignitability requirements were increased. These observations parallel the trends noted in the extinguishment data. In addition to the propellant differences implicitly represented by the burning rate behavior, a rigorous model of propellant extinguishment should include the effect of such variations as binder type and loading level.

Summary

The results of this program showed that the requirements for combustion extinguishment are determined by the propellant formulation, the motor geometry, and, under certain conditions, the exhaust pressure level. The pressure and depressurization rate limits for extinguishment can be altered by formulation differences, variation of the motor geometry, and changing the exhaust atmosphere. A number of trends concerning the effect of formulation differences were established in the course of the following program: 1) The substitution of aluminum for AP in either CTPB or CTPIB propellants decreased the termination requirements, although the tendency for reignition was increased. 2) The addition of burning rate catalysts to a propellant had little or no effect upon the termination requirements in the large-volume small-grain motors used in this program. However, the addition of HYCAT catalyst in aluminized CTPB and CTPIB propellants caused consistent reignition under atmospheric exhaust conditions. 3) The addition of halogens at low concentrations in CTPIB propellants had no effect upon extinguishment limits. 4) Changing the decomposition behavior of the propellant, either by the use of binders (CTPIB) showing lower endothermic thermal decomposition temperatures or by using higher binder levels, resulted in moderate decreases of the extinguishment requirements.

The motor geometry influenced the pressure and depressurization rate at extinguishment. Individually increasing the grain area, decreasing the motor volume, or increasing the termination nozzle throat area of a particular motor will increase the extinguishment pressure and extinguishment depressurization rate. Extinguishment in any particular motor is dependent upon the depressurization path.

The exhaust pressure can influence extinguishment and reignition behavior. When the motor geometry was such that extinguishment occurred below the dechoking pressure, the exhaust pressure influenced the extinguishment limits. Unless the exhaust pressure is below the propellant minimum ignition pressure, reignition may occur, particularly with aluminized propellants.

The von Elbe type of combustion extinguishment model provides a guideline for motor development work. The effects of formulation differences and motor geometry can be adequately considered for preliminary design studies. The effect of exhaust pressure, particularly in regard to reignition behavior, cannot be adequately treated.

References

[1] Fletcher, E. A., Paulson, R. A., Bunde, G. W., and Hiroki, T., "Quenching of Solid Rocket Propellants by Depressurization," WSCI Paper 66-21, presented at Western States Combustion Institute Meeting, April 1966.

[2] Micheli, P. L., "A Stop-Start Study of Solid Propellants," CR-66487, Final Report, Contract No. NAS 1-6600, 1967, NASA.

[3] von Elbe, G. and McHale, E. T., "Extinguishment of Solid Propellants by Rapid Depressurization," *AIAA Journal*, Vol. 6, No. 7, July 1968, pp. 1417–1419.

[4] von Elbe, G., "Theory of Solid Propellant Ignition and Response to Pressure Transients," *Bulletin of the 19th ICRPG Conference*, Silver Spring, Md., 1963, pp. 157–181.

[5] Paul, B. E., Lovine, R. L., and Fong, L. Y., "A Ballistic Explanation of the Ignition Pressure Peak," AIAA Paper 64-121, Palo Alto, Calif., 1964.

[6] Parker, K. H. and Summerfield, M., "Response of the Burning Rate of a Solid Propellant to a Pressure Transient," AIAA Paper 66-683, Colorado Springs, Colo., 1966.

[7] Jensen, G. E., "A Stop-Start Study of Solid Propellants," CR-66488, Final Report, Contract No. NAS 1-6601, 1967, NASA.

[8] Capener, E. L., Dickinson, L. A., and Marxman, G. A., "Propellant Combustion Phenomenon During Rapid Depressurization," Quarterly Report No. 5, Contract No. NAS 7-389, Feb. 1967, Stanford Research Institute, Menlo Park, Calif.

[9] Summerfield, M. and Merkle, G. L., "Extinguishment of Solid Propellant Flames: A Theory on a New Feedback Law," presented at the 3rd ICRPG/AIAA Solid Propulsion Conference, Atlantic City, N.J., 1968.

[10] Jensen, G. E., "An Experimental Study of Solid Propellant Extinguishment by Rapid Depressurization," CR-66747, Final Report, Contract No. NAS 1-7815, March 1969, NASA.

[11] Cheng, J. T., Baer, A. D., and Ryan, N. W., "Thermal Effects of Composite-Propellant Reactions," TR AFOSR 40-66 and 40-67, Aug. 1967, University of Utah, Salt Lake City, Utah.
[12] Madorsky, S. L., *Modern Plastics*, Vol. 38, No. 6, 1961, p. 139.
[13] Jellinek, H. H. G., *Degradation of Vinyl Polymers*, Academic Press, New York, 1955.
[14] Shannon, L. J., "Composite Solid Propellant Ignition Mechanisms," Final Report, Contract No. F44620-68-C-0053, June 1969, United Technology Center, Sunnyvale, Calif.
[15] Shannon, L. J., "Composite Solid Propellant Ignition Mechanisms," AFOSR Scientific Report, AFOSR 67-1765, Contract No. AF 49(638)-1557, Sept. 1967, United Technology Center, Sunnyvale, Calif.

SEPTEMBER 1971 AIAA JOURNAL VOL. 9, NO. 9

Effect of Collisions on Cold Ion Collection by Means of Langmuir Probes

C. H. SHIH* AND E. LEVI†
Polytechnic Institute of Brooklyn, Farmingdale, New York

Langmuir probes are extensively used to sample plasma densities. However, the interpretation of probe data is well established only for the limiting cases of collisionless and collision-dominated plasmas. A transitional regime prevails in some fluid-dynamic situations and electrical discharges in which the ions are colder than the electrons. A simple theory which accounts separately for the effects of collisions between charged particles and collisions with neutrals is presented. When the theory is applied to recent experimental data taken with cylindrical as well as spherical probes, the electron densities calculated from the probe measurements by using the present theory agree within 10% with those inferred from existing numerical solutions, an empirical formula, and microwave cavity data.

Nomenclature

a = radius at last collision
c = aspect ratio
e = electronic charge
E = electric field
I = electric current
I_D = discharge current
J = normalized ion current
k = Boltzmann constant
L = focal distance
L_p = probe length
m = particle mass
n = normalized number density
N = number density
r = spherical radial coordinate
T = temperature
u = radial velocity component
v = normalized ion velocity
V = velocity
w = azimuthal velocity component
x = normalized inverse radius
Z = number of electronic charges
z = cylindrical axial coordinate
α = spherical correction index
β = cylindrical correction index
γ = normalized collision frequency
ζ = spheroidal length coordinate
η = normalized potential
λ = mean free path
λ_D = Debye length
μ = spheroidal angular coordinate
ν = collision frequency
ξ = normalized inverse radius
ρ = cylindrical radial coordinate
φ = potential
ω_p = plasma frequency

Superscripts

o = collisionless A.B.R. theory

Subscripts

c = cylindrical
ca = cavity measurement
e = electron
i = ion
n = neutral
o = sheath edge
p = probe
s = spherical
∞ = far-away from the probe

Received March 30, 1970; presented as Paper 70-757 at the AIAA 3rd Fluid and Plasma Dynamics Conference, Los Angeles, Calif., June 29–July 1, 1970; revision received September 14, 1970. We wish to thank D. M. Bloom for having brought the problem of cold ion collection to our attention and Prof. S. Lederman for having put at our disposal recent unpublished experimental data.[16] We are also grateful to S. A. Self for making available to us the results of his experiments with cylindrical probes. This research has been conducted under Contract Nonr 839(38) and was made possible by the support of the Advanced Research Projects Agency under Order 529 through the Office of Naval Research. This work is taken in part from the dissertation of C. H. Shih submitted to the Faculty of the Polytechnic Institute of Brooklyn in partial fulfillment of the requirements for the degree of Ph.D. (Electrophysics), 1971.

* Graduate Assistant Senior, Electrophysics Department.
† Professor, Electrophysics Department.

I. Introduction

LANGMUIR probes are extensively used to sample plasma densities. For this purpose ion collection is preferable over electron collection because in the former case, the current drawn and, therefore, the perturbation introduced by the probe are much smaller. For a given potential difference between the probe and the plasma, the collected ion current depends strongly on the temperature of the electrons as well as the ions. In most electrical discharges and in many hypersonic testing facilities the ions are much colder than the electrons. As a consequence a great deal of attention has been paid to this particular situation.